



ELSEVIER

Gene Expression Patterns 4 (2004) 351–358



www.elsevier.com/locate/modgep

Glomulin is predominantly expressed in vascular smooth muscle cells in the embryonic and adult mouse

Brendan A.S. McIntyre, Pascal Brouillard, Virginie Aerts,
Ilse Gutierrez-Roelens, Miikka Vikkula*

Laboratory of Human Molecular Genetics, Christian de Duve Institute of Cellular Pathology and Université catholique de Louvain,
Avenue Hippocrate 74 (+5), BP 75.39, 1200 Brussels, Belgium

Received 13 June 2003; received in revised form 28 August 2003; accepted 23 September 2003

Abstract

Mutations in the *glomulin* gene result in dominantly inherited vascular lesions of the skin known as glomuvenous malformations (GVMs). These lesions are histologically distinguished by their distended vein-like channels containing characteristic ‘glomus cells’, which appear to be incompletely or improperly differentiated vascular smooth muscle cells (VSMCs). The function of glomulin is currently unknown. We studied *glomulin* expression during murine development (E9.5 days post-coitum until adulthood) by non-radioactive in situ hybridization. *Glomulin* was first detected at E10.5 dpc in cardiac outflow tracts. Later, it showed strong expression in VSMCs as well as a limited expression in the perichondrium. At E11.5–14.5 dpc *glomulin* RNA was most abundant in the walls of the large vessels. At E16.5 dpc expression was also detectable in smaller arteries and veins. The high expression of *glomulin* in murine vasculature suggests an important role for glomulin in blood vessel development and/or maintenance, which is supported by the vascular phenotype seen in GVM patients with mutations in this gene.

© 2003 Elsevier B.V. All rights reserved.

Keywords: Glomulin; Glomuvenous malformation; Vascular smooth muscle cell; Glomus cell; FAP68; Vasculogenesis; Angiogenesis; Perichondrium; Glomangioma; Glomus tumor

1. Results and discussion

The *glomulin* gene was found by positional cloning (Boon et al., 1999; Brouillard et al., 2000, 2002), to be mutated in autosomal dominantly inherited glomuvenous malformations (GVMs), also known as ‘glomangiomas’, a clinical and radiological subtype of venous malformations (Brouillard and Vikkula, 2003; Vikkula et al., 2001). Most mutations found are presumed to result in truncations of the protein, most likely causing loss-of-function (Brouillard et al., 2002). However, as not all cutaneous veins are affected, the development of lesions is likely to need an additional event. We believe that this results in a complete *localized* loss of glomulin function, as evidenced by a somatic ‘second hit’ identified in the affected tissue of one GVM patient (Brouillard et al., 2002).

Upon histological examination, GVMs are formed of distended vein-like channels containing variable numbers of

poorly differentiated vascular smooth muscle cells (VSMCs), termed ‘glomus cells’, in their walls. Using immunohistochemistry, glomus cells are found to stain positively for smooth muscle cell α -actin and vimentin, but negatively for desmin, von Willebrand factor and S-100 (Kato et al., 1990). In contrast, hereditary mucocutaneous venous malformations, caused by mutations in the angiopoietin receptor TIE-2, are characterized by a relative lack of normally differentiated VSMCs (Vikkula et al., 1996). Clinically, GVM lesions generally take on a purple-blue colored, cobblestone appearance and are painful upon palpation.

Previous studies using the yeast two-hybrid assay have shown full-length glomulin (termed FAP68 by the authors) to associate with the intracellular portion of the proto-oncogene c-Met, also known as hepatocyte growth factor receptor (Grisendi et al., 2001). Another yeast two-hybrid study pulled out a protein with a sequence corresponding to the first three-quarters of the glomulin sequence, which was termed FAP48 for FK506-binding protein associated protein of 48 kDa (Chambraud et al., 1996). This truncated form of glomulin with an altered carboxy-terminal end was

* Corresponding author. Tel.: +32-2-764-7496; fax: +32-2-764-7460.
E-mail address: vikkula@bchm.ucl.ac.be (M. Vikkula).

found to associate with immunophilins FKBP12 and FKBP59 in vitro (Chambraud et al., 1996). Intriguingly, we have not been able to amplify this possible splice variant of *glomulin* from any tested tissues or cells lines.

Full-length human *glomulin* cDNA sequence is present in the Genbank database (accession number CAC82938) and we have sequenced the full-length murine cDNA (accession number AJ566083). In addition, zebrafish ESTs

allowed the assembly of the entire zebrafish *glomulin* cDNA sequence. This was translated and aligned with the full-length murine and human *glomulin* sequences to compare similarities. Sets of complete and incomplete ESTs from all other vertebrates in which a *glomulin* orthologue was found were also aligned and a cladogram is shown in Fig. 1A. Overall, the amino acid sequence identity between human and murine *glomulin* is 87%, but only 49% between human

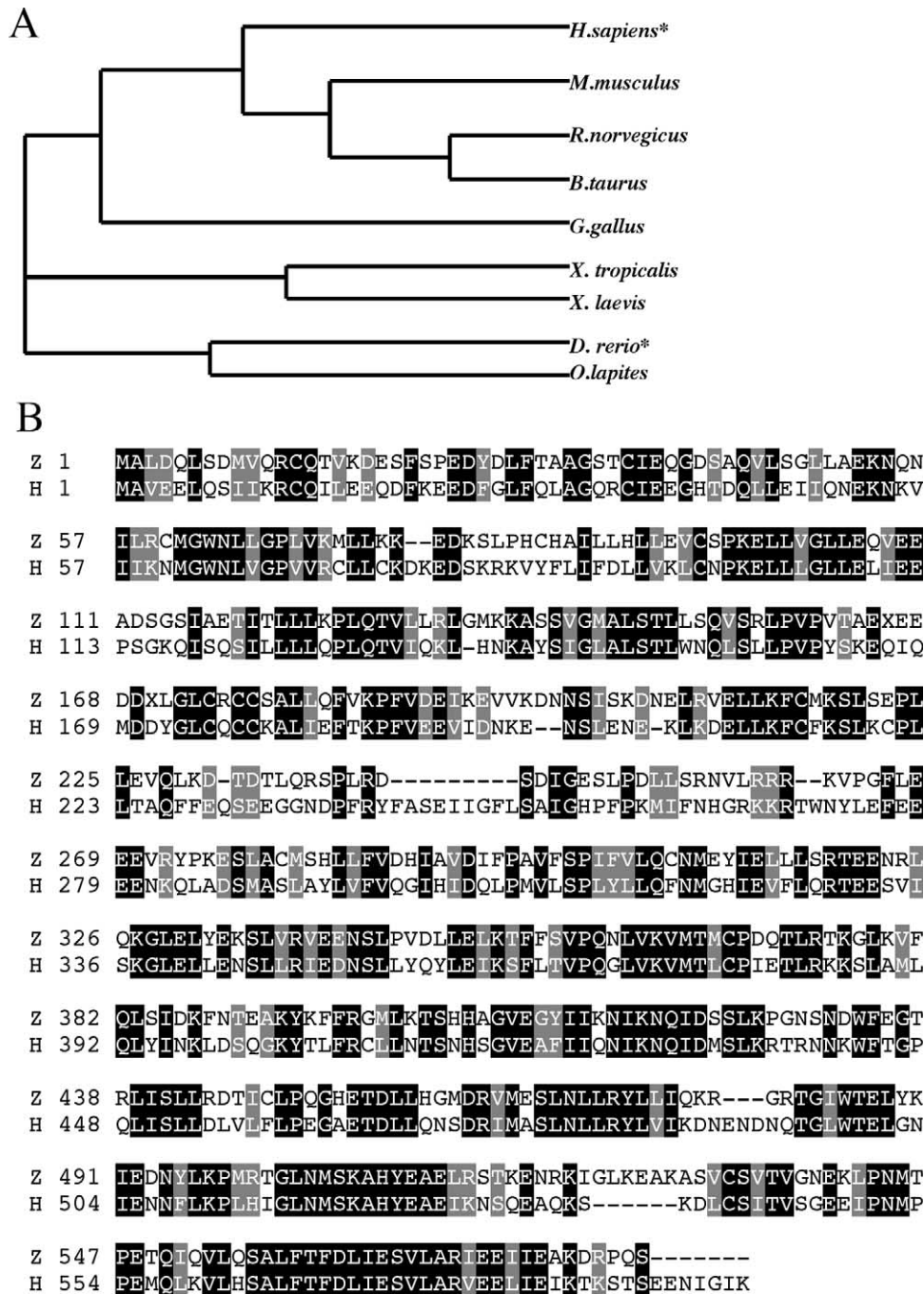


Fig. 1. (A) Cladogram generated by ClustalW showing the degree of similarity between *glomulin* amino acid sequences from *H. sapiens** and *M. musculus* aligned with translated ESTs from *R. norvegicus*, *B. taurus*, *G. gallus*, *X. tropicalis*, *X. laevis*, *D. erio* (zebrafish)*, and *O. lapites* (guppy). *Alignment of these two full-length sequences is shown below. (B) Boxshade graphical output of ClustalW alignment of full-length human, H and zebrafish, Z sequences. Black, identical; gray, conserved change.

and zebrafish. When comparing homology, these numbers are raised to 90% and 62%, respectively. Interestingly, the homology between the human and the zebrafish sequence is poor in the middle of the sequence (amino acid 226–266), which includes a nine amino acid gap starting at residue 242, but is well conserved at both ends. Furthermore, the zebrafish sequence is terminated seven amino acids earlier than both the human and murine sequences (Fig. 1B). When examining the 3'UTR, a second in-frame TAA Stop codon is found 24 nucleotides after the human Stop codon and 12 nucleotides after the murine Stop codon. A second in-frame TGA Stop codon is found six nucleotides after the zebrafish Stop codon. Screening for conserved functional domains

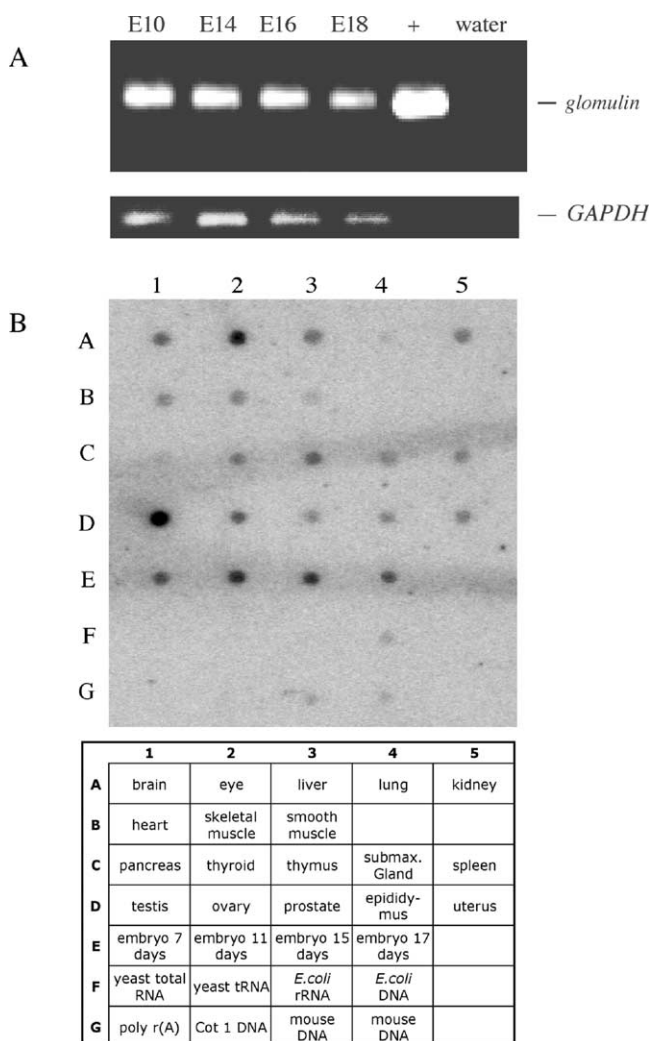


Fig. 2. (A) *Glomulin*-specific RT-PCR using cDNA from whole murine embryos from E10 to E18. Glyceraldehyde-3-phosphate dehydrogenase (GAPDH) was amplified to control for presence of cDNA in each reaction. Positive control (+) for the *glomulin* RT-PCR was a pBluescript clone containing full-length murine *glomulin*. This sample is negative for GAPDH. Water was used as negative control. (B) Clontech Mouse RNA Master Blot probed with a radiolabeled *glomulin* probe. All spots derived from RNA extracted from murine tissues are positive. Negative controls from microorganisms, poly-A RNA, and Cot-1 DNA are negative. Murine, and *E. coli* DNA give a weak positive signal. Source of are RNAs indicated below.

using PredictProtein and SMART only identified a few potential phosphorylation and glycosylation sites (data not shown). As no signal sequence or clear transmembrane domain was identified, *glomulin* is likely an intracellular protein.

In the human adult, *glomulin* is expressed at high levels in skeletal muscle, heart, brain and kidney, and at low levels in all other organs on the basis of Northern blot hybridizations (Brouillard et al., 2002). Nothing is known about the expression pattern of *glomulin* during embryogenesis, nor of the identity of the cells expressing *glomulin*. As an initial test for developmental *glomulin* expression we used total embryonic RNA as template for cDNA synthesis and polymerase chain reaction (RT-PCR). *Glomulin* amplicons were observed in cDNA from embryos at E10, E14, E16 and E18 days post-coitum (dpc) (Fig. 2A). Additionally, a murine dot blot shows a ubiquitous presence of *glomulin* mRNA in murine tissues (Fig. 2B).

For more precise localization of the developmental and adult expression of *glomulin*, non-radioactive RNA in situ hybridization (RNA ISH) was used. Two short *glomulin* probes and one long *glomulin* probe were synthesized for use in RNA ISH (see Section 2). Only the long probe gave strong positive signal and was hence used throughout the study. A murine *desmin* probe was used as a control and showed a strong staining of skeletal muscle with weaker staining of cardiac and VSMCs, in accordance with previous observations (Figs. 3A,4B,D,5G,6B; Raguz et al., 1998). A *glomulin* sense probe was used as a negative control, and no hybridization with this probe was observed unless otherwise stated. Embryos from E9.5 to E16.5 and adult tissues were studied. *Glomulin* expression became evident only at E10.5, when it was seen in the third branchial arch artery, and the third branchial pouch (Fig. 3B–E), a signal that was confirmed in multiple hybridizations of different embryos. Upon examination of sagittal and transverse sections of embryonic stages from E11.5 to E16.5, *glomulin* expression was observed in large veins and arteries of the cardio-pulmonary trunk, including the aortic arch, branchial arch arteries, carotid arteries, descending thoracic aorta, dorsal aorta, ductus arteriosus, left fourth aortic arch arteries, pulmonary arteries, subclavian arteries, right fourth aortic arch arteries, and the vena cava (Fig. 4A,C,E–G). Sagittal sections from E11.5 (Fig. 4A) and E14.5 (Fig. 4C) embryos showed specific staining throughout the length of the dorsal aorta and descending thoracic aorta, respectively.

Glomulin expression in the vasculature was observed to be exclusive to VSMC when examining large vessels in E14.5, E16.5 and the adult (Fig. 5A–F). *Glomulin* expression was restricted to the walls of the E14.5 brachiocephalic artery and right superior vena cava (Fig. 5A–C). At E16.5 we could observe a thick wall of stained VSMCs in the right and left carotid arteries, arch of the aorta and pulmonary artery (Fig. 5D,E). Most distinct, however, was the expression observed in the adult thoracic aorta where a clear non-stained endothelial cell layer was

observed luminal to the VSMC containing intima (Fig. 5F). In earlier stages this distinction was limited due to the size of the vessel wall.

VSMCs are first recognized in the dorsal aorta at E9.5 (Parmacek, 2001). The first marker of the smooth muscle cell lineage, smooth muscle α -actin, is expressed in this structure at stage 12 (16 somites) in chicken (Owens, 1995). This developmental time point corresponds to E9–9.5 in the mouse. Smooth muscle cell α -actin expression is followed by SM-22, calponin, h-caldesmon and smooth muscle α -tropomyosin expression (Owens, 1995). Glomulin expression begins at E10.5, at the same developmental time point as smooth muscle myosin heavy chain (E10.5 murine), and just before the late VSMC developmental marker smoothelin (chicken stage 20, corresponding to E11 murine) (Deruiter et al., 2001; Owens, 1995). Interestingly, glomus cells present in GVMs lack expression of desmin, a marker of differentiated muscle cells. This absence could be due to the lack of glomulin that may be needed for the differentiation of VSMCs and thus for the expression of desmin.

Glomulin expression was also observed in the perichondrium around sites of rib, vertebra and long bone development of E14.5 embryos (Fig. 6A). *Glomulin*

expression was either no longer present or severely diminished at these sites by E16.5 (Fig. 6C). The trachobronchial lining was also positive at E14.5 (Fig. 6A), as was the elastic tissue and smooth muscle (trachealis smooth muscle) in the posterior third of the trachea at E16.5 (Figs. 4G,5D). As such, this staining pattern is reminiscent of in situ hybridization studies of the embryonic vascular EGF-like repeat containing protein (EVEC) and the latent TGF- β binding protein-2 (LTBR2) genes, which exhibit embryonic expression in VSMCs and a transient expression in the perichondrium (Kowal et al., 1999; Fang et al., 1997).

The kidney is an organ that was previously demonstrated to have elevated levels of *glomulin* mRNA (Brouillard et al., 2002). Consistent with this finding, we observed strong, specific *glomulin* staining of arteries within the parenchyma of the adult kidney (Fig. 7A,B). In other adult organs, such as the lung, *glomulin* expression was also observed within vessel walls (data not shown). Interestingly, hair follicles and vibrissae (whiskers) in adult and neonate skin seemed to stain specifically for *glomulin*, yet these structures also gave weak positive results with the *glomulin* sense probe (Fig. 8A,B).

In summary, *glomulin* expression was seen within the large vessels of the developing vasculature and at sites of

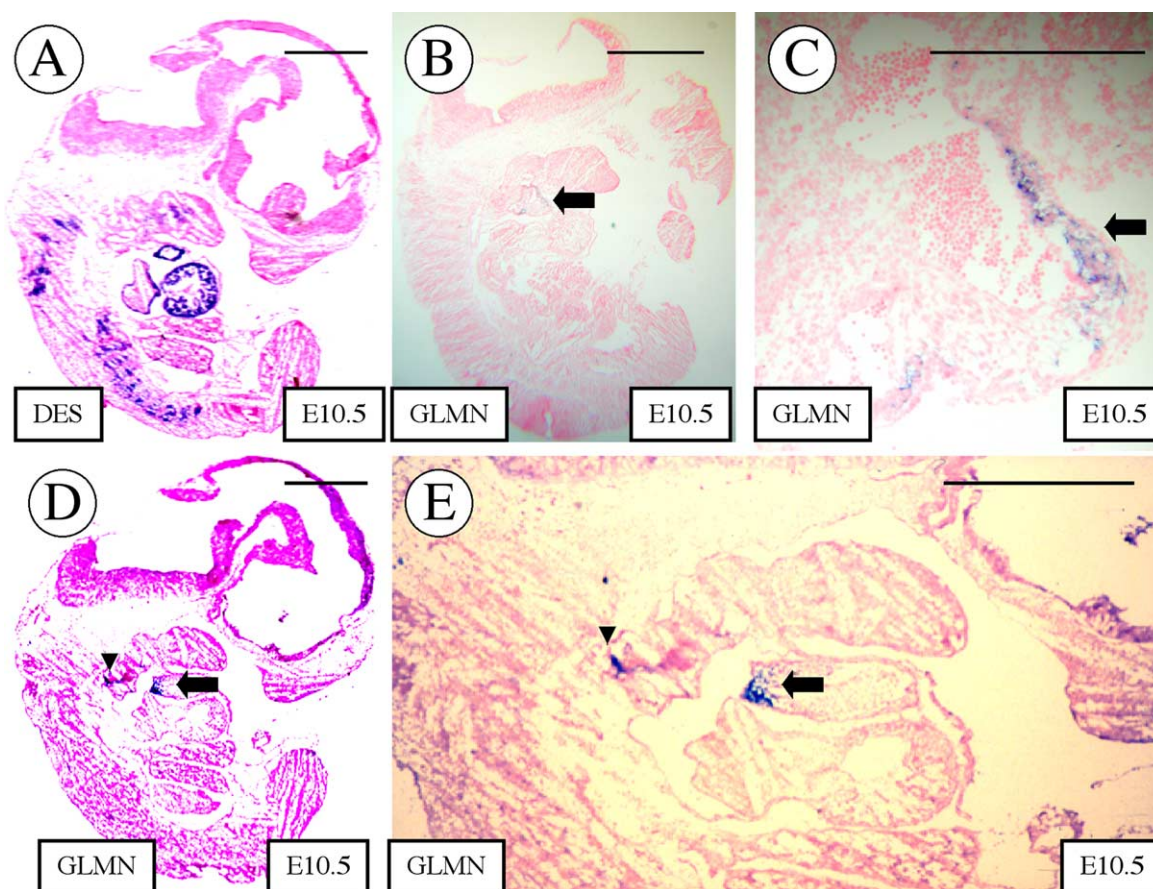
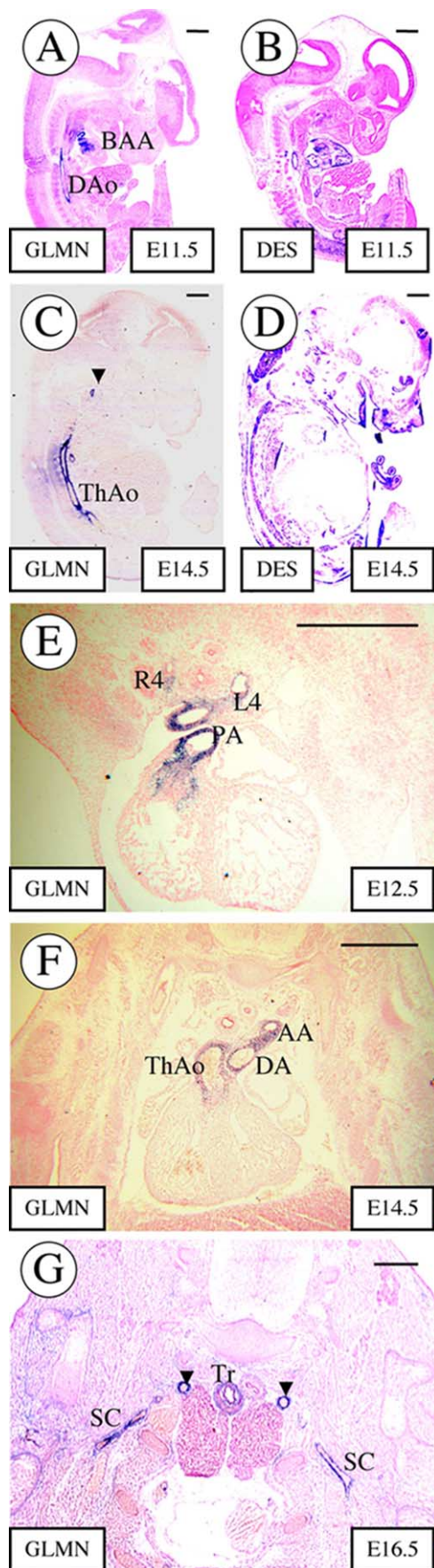


Fig. 3. *Glomulin* expression in sagittal sections of E10.5 embryos. (A) Somites and primitive heart are stained. (B–E) C is a magnification of B and E is a magnification of D. Arrows indicate third branchial arch artery; arrowheads indicate third branchial pouch. All sections counterstained with Nuclear Fast Red. Bars for A,B,D,E, 500 μ m; bar for C, 250 μ m. (A) DES, *desmin*; (B–E) GLMN, *glomulin*.



chondrogenesis in the embryo; while vascular expression of *glomulin* persisted in the adult, it was transient at sites of endochondral bone formation. The expression pattern of *glomulin* indicates that GVMs are due to a primary defect in VSMCs and not in vascular endothelial cells. This differs from mucocutaneous venous malformations, VMCM (Boon et al., 1994), which are caused by gain-of-function mutations in the angiopoietin receptor TIE-2, expressed in vascular endothelial cells (Vikkula et al., 1996). Glomulin is thus likely an important factor for VSMC differentiation, as suggested by the altered VSMC phenotype of glomus cells in GVMs.

2. Methods

2.1. Sequence comparisons and assembly

Species specific *glomulin* cDNA sequences were compiled by performing tblastn using human and murine glomulin protein sequences against EST databases (<http://www.ncbi.nlm.nih.gov/BLAST>). Sequence alignments and cladogram generation was performed using ClustalW (<http://www.ebi.ac.uk/clustalw>). Graphical output of ClustalW alignments was generated using Boxshade (<http://www.ch.embnet.org>). Domain prediction was performed by using the Simple Modular Architecture Research Tool or SMART (<http://dag.embl-heidelberg.de>) and PredictProtein (<http://www.embl-heidelberg.de/predictprotein>).

2.2. cDNA synthesis and PCR amplification

The SuperScript Preamplification System for First Strand cDNA Synthesis kit was used to create cDNA using a poly-T primer (Invitrogen Life Technologies). Amplicons were created using murine *glomulin* specific or glyceraldehyde-3-phosphate dehydrogenase (GAPDH) control gene-specific primers (primer sequences available on request). All amplicons span multiple exon–intron boundaries.

2.3. RNA dot blot

Hybridization of the Mouse RNA Master Blot (Clontech) was performed according to the supplied protocol. The blot

← Fig. 4. *Glomulin* expression in the large vessels of E11.5–E16.5 embryos. (A–D) Sagittal sections. (E–G) Transverse sections hybridized with *glomulin* probes at E12.5, E14.5 and E16.5, respectively. AA, aortic arch; BAA, branchial arch arteries; DA, ductus arteriosus; DAo, dorsal aorta; L4, left fourth aortic arch artery; PA, pulmonary artery; R4, right fourth aortic arch artery; SC, subclavian arteries; ThAo, thoracic aorta; Tr, trachea; arrowheads indicate carotid arteries (C and G). Sections A, B, E–G counterstained with Nuclear Fast Red. Bars, 500 μm. (A,C,E–G) GLMN, (B,D) DES.

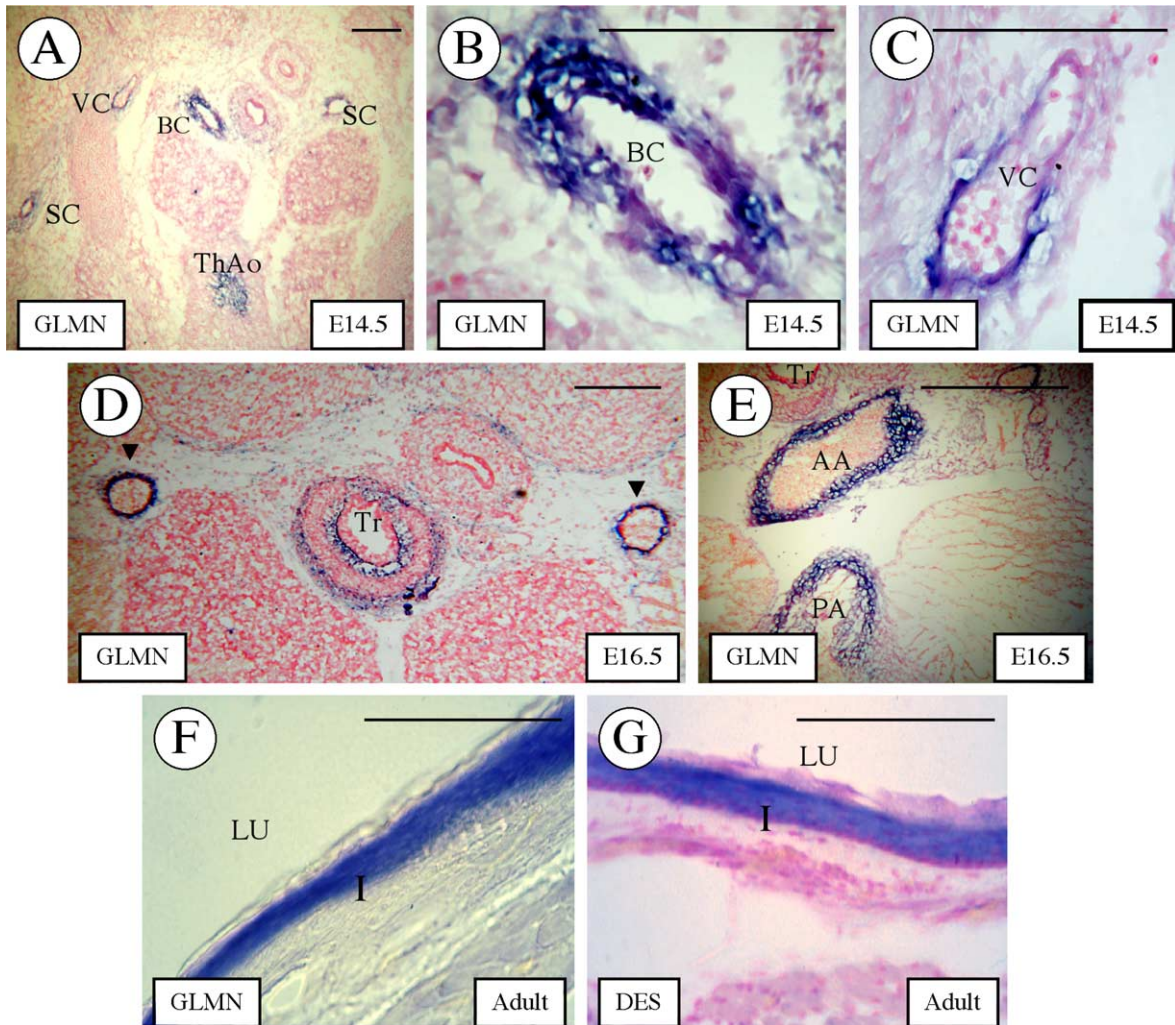


Fig. 5. *Glomulin* expression in VSMCs. Transverse sections through midline of E14.5 (A–C) and E16.5 embryos (D,E). B and C are magnifications of the indicated vessels in A. (F,G) High magnification of the wall of adult aorta. AA, aortic arch; BC, brachiocephalic artery; I, intima; LU, lumen; PA, pulmonary artery; SC, subclavian arteries; ThAo, thoracic aorta (origin); Tr, trachea; VC, vena cava; arrowheads indicate carotid arteries (D). All sections except (F) counterstained with Nuclear Fast Red. Bars, 250 μ m. (A–F) GLMN, (G) DES.

was probed with a radiolabeled 1640 nt sequence covering position 1–1640 in the coding region of the murine *glomulin* cDNA. Radiolabeling was generated using random priming with α P-[32]dCTP. The hybridized blot was exposed to Biomax films for visualization (Kodak).

2.4. Animals and tissues

Studies have been approved by the ethics committee of the Université catholique de Louvain and have been carried out in accordance with NIH guidelines on animal ethics. CD1 mice were mated overnight and the morning of vaginal plug detection was considered to be day 0.5 post-coitum (dpc). Embryos and organs of newborn and adult mice used for RNA-ISH were removed and fixed overnight at 4 °C in 4% paraformaldehyde in phosphate buffered saline (PBS). The samples were subsequently incubated in RNase-free 20% sucrose in PBS at 4 °C for at least 4 h, embedded in

Tissue-Tek (Labonord) and stored at –80 °C. Embedded embryos and whole organs were cut on a Leitz cryostat. Sections ranging from 10 to 14 μ m were mounted on Superfrost slides (Labonord).

2.5. RNA in situ hybridization

For the long *glomulin* probe, a 1162 nt sequence, containing the last 1132 nt of the ORF and the first 30 nt of the 3'UTR, was cloned in sense orientation into pBluescript (Stratagene). A second, smaller set of *glomulin* probes were generated using a 278 nt fragment from position 919 to 1197 in the ORF, and a 353 nt fragment from position 1425 to 1778 in the ORF. A positive control probe, containing the last 34 nt of the coding sequence and the 3'UTR of *desmin*, also cloned in sense orientation in pBluescript, was kindly provided by Dr Michael Antoniou (Department of Experimental Pathology, UMDS, Guy's

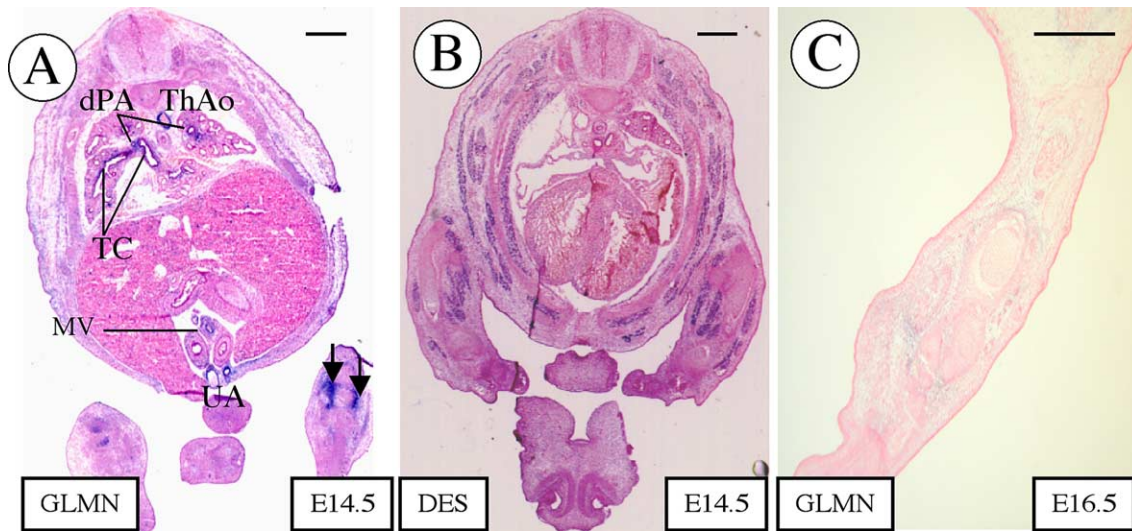


Fig. 6. *Glomulin* expression in the perichondrium of E14.5 and E16.5 embryos. Transverse sections of E14.5 embryos (A,B), and forelimb of E16.5 embryo (C). Note strong *glomulin* expression in the perichondrium at E14.5 (arrows) versus weak expression at E16.5. dPA, distal pulmonary arteries; MV, mesenteric vitelline vessels; TC, tracheobronchial lining; ThAo, thoracic aorta; UA, umbilical arteries; arrows, perichondrium of longbones. All sections counterstained with Nuclear Fast Red. Bars, 500 μ m. (A,C) GLMN, (B) DES.

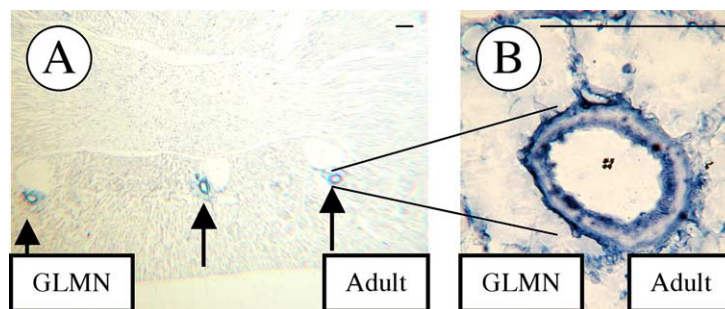


Fig. 7. *Glomulin* expression in the adult kidney. (A,B) Sagittal section through the kidney. Arrows indicate arteries located in the parenchyma of the kidney. Bars, 250 μ m.

Hospital, London Bridge, London). Vectors were linearized using *Bam* H I and *Hind* III for *glomulin*, and *Xho* I and *Not* I for *desmin*, sense and antisense, respectively. Probes were synthesized using T3 (sense) or T7 (antisense) RNA polymerase and DIG-UTP (Roche). After synthesis, 1 μ l of each probe was denatured, separated by agarose gel electrophoresis, and photographed. Prior to hybridization, slides were washed in PBS, [0.3%] Triton X-100 and twice in PBS at 67 $^{\circ}$ C. Hybridization was carried out at 67 $^{\circ}$ C overnight in a buffered solution containing 50% formamide, yeast rRNA (1 mg/ml), 1 \times Denhardt's solution, and 10% dextran sulfate. Post-hybridization washes were in 1 \times SSC, 50% formamide and 0.1% Tween-20 at 67 $^{\circ}$ C, and Tris-buffered saline 0.1% Tween (TBS-T). Incubation with Roche anti-DIG-AP Fab fragments diluted 1:500 in Roche blocking reagent was performed overnight at room temperature. After washing four times in TBS-T and twice in alkaline phosphatase staining buffer containing 5 mM levamisole phosphatase inhibitor, slides were incubated at 37 $^{\circ}$ C with alkaline phosphatase staining buffer containing NBT-BCIP. Signal enhancement was obtained by using

10% w/v high molecular weight polyvinyl alcohol, as described by DeBlock and colleagues (DeBlock and Debrouwer, 1993). When indicated, counterstaining was performed using Nuclear Fast Red (Dako).

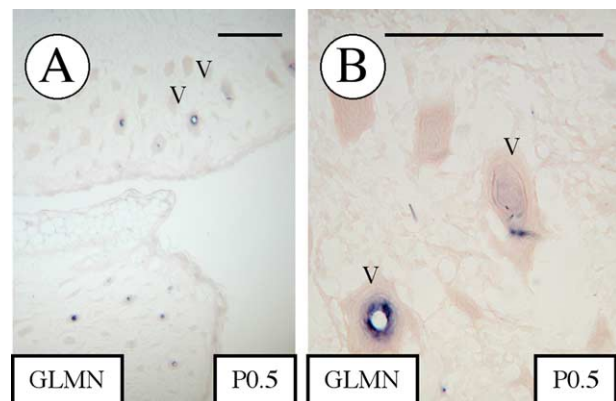


Fig. 8. *Glomulin* expression in vibrissae of P0.5 neonates. (A,B) Sagittal sections through the upper and lower snout. V, vibrissa. Bars, 250 μ m.

Acknowledgements

B.A.S.M. has been supported by the Fonds Spéciaux de Recherche-Université catholique de Louvain, and is currently the recipient of a Doctoral Research Grant from the National Science and Engineering Research Council of Canada (NSERC). P.B. was supported by a fellowship from the Fonds pour la formation à la recherche dans l'industrie et dans l'agriculture (FRIA). These studies were supported by the Belgian Federal Service for Scientific, Technical and Cultural Affairs; Actions de Recherche Concertées—Communauté française de Belgique (ARC); and the Fonds National de la Recherche Scientifique (support to M.V., a 'chercheur qualifié du FNRS'). Embryonic cDNA samples for RT-PCR were kindly supplied by Mr Mathieu Bertrand. We thank Ms Ana Gutierrez for excellent technical help and Ms Liliana Niculescu for secretarial and administrative work.

References

- Boon, L.M., Mulliken, J.B., Vikkula, M., Watkins, H., Seidman, J., Olsen, B.R., Warman, M.L., 1994. Assignment of a locus for dominantly inherited venous malformations to chromosome 9p. *Hum. Mol. Genet.* 3, 1583–1587.
- Boon, L.M., Brouillard, P., Irrthum, A., Karttunen, L., Warman, M.L., Rudolph, R., et al., 1999. A gene for inherited cutaneous venous anomalies (glomangiomas) localizes to chromosome 1p21-22. *Am. J. Hum. Genet.* 65 (1), 125–133.
- Brouillard, P., Vikkula, M., 2003. Vascular malformations: localized defects in vascular morphogenesis. *Clin. Genet.* 63 (5), 340–351.
- Brouillard, P., Olsen, B.R., Vikkula, M., 2000. High-resolution physical and transcript map of the locus for venous malformations with glomus cells (VMGLOM) on chromosome 1p21-p22. *Genomics* 67 (1), 96–101.
- Brouillard, P., Boon, L.M., Mulliken, J.B., Enjorlas, O., Ghassibe, M., Warman, M.L., et al., 2002. Mutations in a novel factor, glomulin, are responsible for glomovenous malformations (glomangiomas). *Am. J. Hum. Genet.* 70 (4), 866–874.
- Chambrud, B., Radanyi, C., Camonis, J.H., Shazand, K., Rajkowski, K., Baulieu, E.E., 1996. FAP48, a new protein that forms specific complexes with both immunophilins FKBP59 and FKBP12. Prevention by the immunosuppressant drugs FK506 and rapamycin. *J. Biol. Chem.* 271 (51), 32923–32939.
- DeBlock, M., Debrouwer, D., 1993. RNA–RNA in situ hybridization using digoxigenin-labeled probes: the use of high molecular weight polyvinyl alcohol in the alkaline phosphatase indoxyl-nitroblue tetrazolium. *Anal. Biochem.* 216, 88–89.
- Deruiter, M.C., Rensen, S.S., Coolen, G.P., Hierck, B.P., Bergwerff, M., Debie, W.M., et al., 2001. Smoothelin expression during chicken embryogenesis: detection of an embryonic isoform. *Dev. Dyn.* 221 (4), 460–463.
- Fang, J., Li, X., Smiley, E., Francke, U., Mecham, R.P., Bonadio, J., 1997. Mouse latent TGF- β binding protein-2: molecular cloning and developmental expression. *Biochim. Biophys. Acta* 1345, 219–230.
- Grisendi, S., Chambrud, B., Gout, I., Comoglio, P.M., Creparli, T., 2001. Ligand-regulated binding of FAP68 to the hepatocyte growth factor receptor. *J. Biol. Chem.* 276 (49), 46632–46638.
- Kato, N., Kumakiri, M., Ohkawara, A., 1990. Localized form of multiple glomus tumors: report of the first case showing partial involution. *J. Dermatol.* 17, 423–438.
- Kowal, R.C., Richardson, J.A., Miano, J.M., Olson, E.N., 1999. EVEC, a novel epidermal growth factor-like repeat-containing protein upregulated in embryonic and diseased adult vasculature. *Circ. Res.* 84, 1166–1176.
- Owens, G.K., 1995. Regulation of differentiation of vascular smooth muscle cells. *Physiol. Rev.* 75, 487–517.
- Parmacek, M.S., 2001. Transcriptional programs regulating vascular smooth muscle cell development and differentiation. *Curr. Top. Mol. Biol.* 51, 69–89.
- Raguz, S., Hobbs, C., Yagüe, E., Ioannou, P.A., Walsh, F.S., Antoniou, M., 1998. Muscle-specific locus control region activity associated with the human desmin gene. *Dev. Biol.* 201, 26–42.
- Vikkula, M., Boon, L.M., Carraway, K.L. III, Calvert, J.T., Diamonti, A.J., Goumnerov, B., 1996. Vascular dysmorphogenesis caused by an activating mutation in the receptor tyrosine kinase TIE2. *Cell* 87, 1181–1190.
- Vikkula, M., Boon, L.M., Mulliken, J.B., 2001. Molecular genetics of vascular malformations. *Matrix Biol.* 20 (5–6), 327–335.